Supporting Information for

Tuning the electronic and optical properties of hg-C$_3$N$_4$ quantum dots with edge-functionalization: A computational perspective

Khushboo Dange, Vaishali Roondhe, and Alok Shukla*

Department of Physics, Indian Institute of Technology Bombay, Powai, Mumbai 400076, India

This supporting information is divided into four sections. The first section contains the calculated bond lengths and bond angles for the considered structures. The second section contains the discussion on their Raman spectra and some unique vibrational modes. The third section contains the plots of total density of states (TDOS) and partial density of states (PDOS) for the pristine and edge-functionalized hg-C$_3$N$_4$ QDs. The last section contains the UV-vis absorption spectra for all the pristine structures and the information related to the excited states contributing to the most intense peaks in the absorption spectra as well as the first excited state of all the structures considered in this work.

A. Bond lengths and bond angles

Table S1: Calculated bond lengths and bond angles for the atoms that are nearby the attached functional groups for all the considered structures.

Structure	Bond Lengths	Cal. (Å)	Bond Angles	Cal. (°)	Structure	Bond Lengths	Cal. (Å)	Bond Angles	Cal. (°)
1-Pris	C4-N16	1.35	N16-C4-N8	116.0	4-COOH	C33-N43	1.38	N43-C33-N36	119.3
	C4-N8	1.34	N16-C4-N7	116.0		C33-N37	1.34	N43-C33-N37	112.1
	C4-N7	1.34	N7-C4-N8	127.9		C33-N36	1.33	N37-C33-N36	128.6
1-CH$_3$	C4-N16	1.35	N16-C4-N8	114.8	4-OH	C33-N43	1.34	N43-C33-N36	114.6
	C4-N8	1.34	N16-C4-N7	117.8		C33-N37	1.35	N43-C33-N37	116.5
	C4-N7	1.35	N7-C4-N8	127.4		C33-N36	1.39	N37-C33-N36	128.8
1-CHO	C4-N16	1.38	N16-C4-N8	112.2	4-F	C33-N43	1.38	N43-C33-N36	118.3
	C4-N8	1.34	N16-C4-N7	119.1		C33-N37	1.33	N43-C33-N37	111.8
	C4-N7	1.32	N7-C4-N8	128.7		C33-N36	1.34	N37-C33-N36	129.7
1-COCH$_3$	C4-N16	1.38	N16-C4-N8	112.0	5-Pris	C50-N62	1.34	N62-C50-N59	115.9
	C4-N8	1.34	N16-C4-N7	119.6		C50-N61	1.35	N62-C50-N61	115.9
	C4-N7	1.33	N7-C4-N8	128.4		C50-N59	1.35	N61-C50-N59	128.1
1-COOH	C4-N16	1.38	N16-C4-N8	112.0	5-CH$_3$	C50-N62	1.34	N62-C50-N59	117.7
	C4-N8	1.34	N16-C4-N7	119.3		C50-N61	1.35	N62-C50-N61	117.7
	C4-N7	1.33	N7-C4-N8	128.7		C50-N59	1.35	N61-C50-N59	127.5

1-OH	C4-N16	1.35	N16-C4-N8	116.5	5-CHO	C50-N62	1.38	N62-C50-N59	118.9
	C4-N8	1.34	N16-C4-N7	114.7		C50-N61	1.34	N62-C50-N61	112.2
	C4-N7	1.34	N7-C4-N8	128.8		C50-N59	1.33	N61-C50-N59	128.8
1-F	C4-N16	1.39	N16-C4-N8	111.7	5-COCH$_3$	C50-N62	1.38	N62-C50-N59	119.5
	C4-N8	1.34	N16-C4-N7	118.3		C50-N61	1.35	N62-C50-N61	112.0
	C4-N7	1.32	N7-C4-N8	129.8		C50-N59	1.33	N61-C50-N59	128.5
3-Pris	C18-N30	1.34	N30-C18-N27	115.9	5-COOH	C50-N62	1.38	N62-C50-N59	119.1
	C18-N27	1.35	N30-C18-N29	116.0		C50-N61	1.34	N62-C50-N61	112.1
	C18-N29	1.35	N27-C18-N29	128.0		C50-N59	1.33	N61-C50-N59	128.8
3-CH$_3$	C18-N30	1.34	N30-C18-N27	114.7	5-OH	C50-N62	1.34	N62-C50-N59	114.6
	C18-N27	1.35	N30-C18-N29	117.8		C50-N61	1.34	N62-C50-N61	116.4
	C18-N29	1.35	N27-C18-N29	127.4		C50-N59	1.35	N61-C50-N59	129.0
3-CHO	C18-N30	1.38	N30-C18-N27	112.2	5-F	C50-N62	1.38	N62-C50-N59	118.2
	C18-N27	1.35	N30-C18-N29	119.0		C50-N61	1.34	N62-C50-N61	111.7
	C18-N29	1.33	N27-C18-N29	128.7		C50-N59	1.33	N61-C50-N59	129.9
3-COCH$_3$	C18-N30	1.38	N30-C18-N27	112.0	6-Pris	C85-N97	1.34	N97-C85-N89	116.1
	C18-N27	1.35	N30-C18-N29	119.5		C85-N88	1.35	N97-C85-N88	115.9
	C18-N29	1.33	N27-C18-N29	128.4		C85-N89	1.35	N89-C85-N88	128.0
3-COOH	C18-N30	1.38	N30-C18-N27	112.0	6-CH$_3$	C85-N97	1.34	N97-C85-N89	117.9
	C18-N27	1.35	N30-C18-N29	119.3		C85-N88	1.35	N97-C85-N88	114.7
	C18-N29	1.33	N27-C18-N29	128.7		C85-N89	1.35	N89-C85-N88	127.4
3-OH	C18-N30	1.34	N30-C18-N27	116.4	6-CHO	C85-N97	1.38	N97-C85-N89	119.0
	C18-N27	1.35	N30-C18-N29	114.6		C85-N88	1.35	N97-C85-N88	112.3
	C18-N29	1.35	N27-C18-N29	128.9		C85-N89	1.33	N89-C85-N88	128.7
3-F	C18-N30	1.38	N30-C18-N27	111.7	6-COCH$_3$	C85-N97	1.38	N97-C85-N89	119.6
	C18-N27	1.34	N30-C18-N29	118.4		C85-N88	1.35	N97-C85-N88	112.6
	C18-N29	1.33	N27-C18-N29	129.8		C85-N89	1.33	N89-C85-N88	128.4
4-Pris	C33-N43	1.34	N43-C33-N36	116.0	6-COOH	C85-N97	1.38	N97-C85-N89	119.3
	C33-N37	1.35	N43-C33-N37	116.0		C85-N88	1.35	N97-C85-N88	112.6
	C33-N36	1.35	N37-C33-N36	128.0		C85-N89	1.33	N89-C85-N88	128.6
4-CH$_3$	C33-N43	1.35	N43-C33-N36	117.8	6-OH	C85-N97	1.34	N97-C85-N89	114.6
	C33-N37	1.35	N43-C33-N37	114.8		C85-N88	1.35	N97-C85-N88	116.4
	C33-N36	1.34	N37-C33-N36	127.4		C85-N89	1.35	N89-C85-N88	128.9
4-CHO	C33-N43	1.38	N43-C33-N36	119.0	6-F	C85-N97	1.38	N97-C85-N89	118.4
	C33-N37	1.34	N43-C33-N37	112.3		C85-N88	1.34	N97-C85-N88	111.7
	C33-N36	1.33	N37-C33-N36	128.6		C85-N89	1.33	N89-C85-N88	129.8
4-COCH$_3$	C33-N43	1.38	N43-C33-N36	119.6					
	C33-N37	1.35	N43-C33-N37	112.1					
	C33-N36	1.33	N37-C33-N36	128.3					

B. Vibrational Properties: Raman Spectra

The computed Raman spectra corresponding to each of the considered structures is depicted in Fig. S1. The peaks in each of the plots can be classified into two regions: (i) the low-intensity region and (ii) the high-intensity region. As shown in Fig. S1(b), the low intensity peaks for all the considered 3−X structures fall in the frequency range 700−1700 cm^{-1}, which arise mostly due to the deformation of C−N bonds because of their stretching and scissoring modes. In the frequency range 3000−4000 cm^{-1}, peaks arise due to stretching vibrations of the N−H bonds, with the highest intensity near 3600 cm^{-1}. In addition to these, peaks corresponding to unique vibrational modes of the bonds

of the attached functional groups are also present in the spectra of functionalized hg-C_3N_4 QDs. In the Raman spectra of 3-CH_3 QD, stretching of the C-H bonds (of -CH_3) gives rise to a peak at 3000 cm^{-1}. For 3-CHO QD, vibrations due to stretching of C=O and C-H bonds are also present at the frequencies 1840 cm^{-1} and 2920 cm^{-1}, respectively. Similarly, in the case of 3-$COCH_3$ structure, stretching of the C=O bond occurs at 1837 cm^{-1} whereas stretching of the C-H bonds occur in the frequency range 3000−3100 cm^{-1}. In the case of 3-COOH structure, vibrations due to the attached functional group are present around 1870 cm^{-1} which include stretching of the C=O and O-H bonds as well as scissoring of the O-C=O bond. In the Raman spectra of 3-OH and 3-F QDs, peaks around 3500 cm^{-1} correspond to stretching of the O-H and O-F bonds, respectively. The Raman spectra of other pristine hg-C_3N_4 QDs and their associated functionalized structures exhibit similar type of qualitative behavior, as illustrated in Figs. S1(a), (c), (d), and (e).
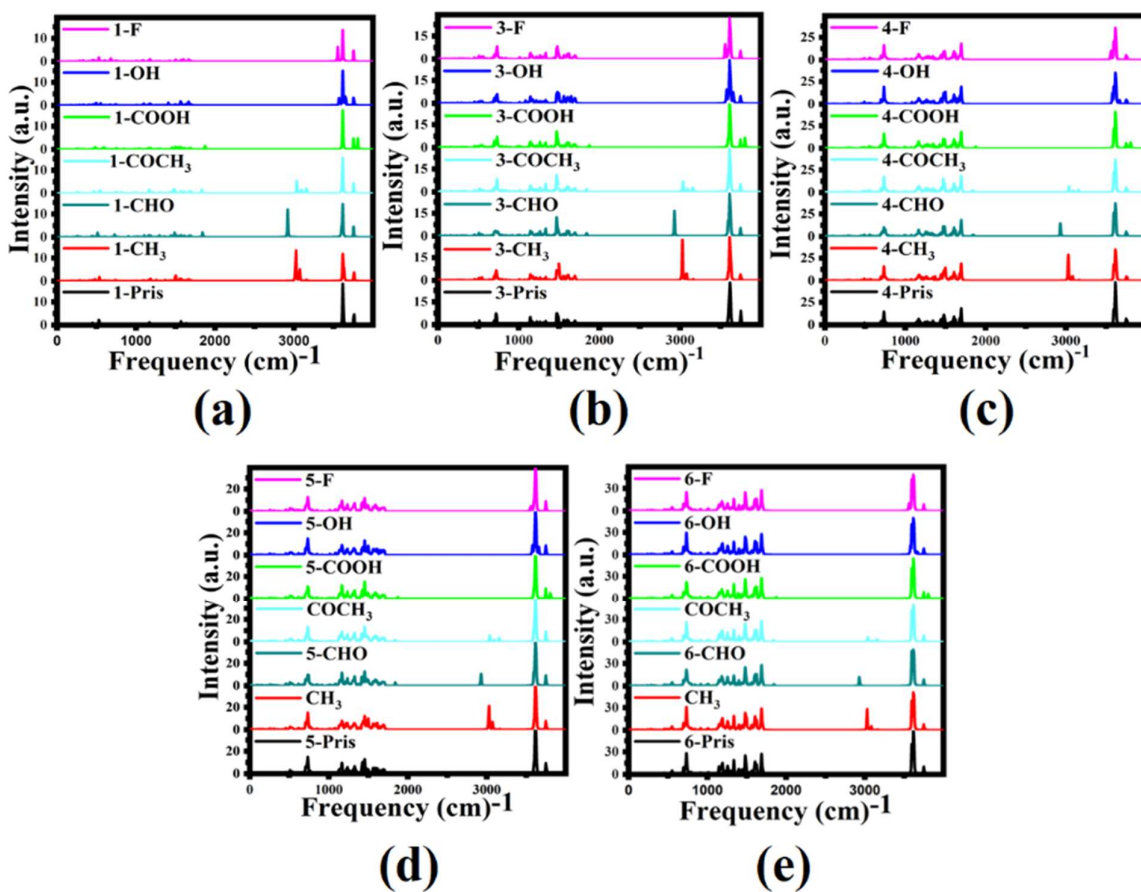

Figure S1: Raman spectra plots of (a) 1−X, (b) 3−X, (c) 4−X, (d) 5−X, and (e) 6−X structures. X represents the attached functional groups ($-Pris$, $-CH_3$, $-CHO$, $-COCH_3$, $-COOH$, $-OH$, and $-F$).

C. Total and partial density of states plots for the considered hg-C₃N₄ quantum dots
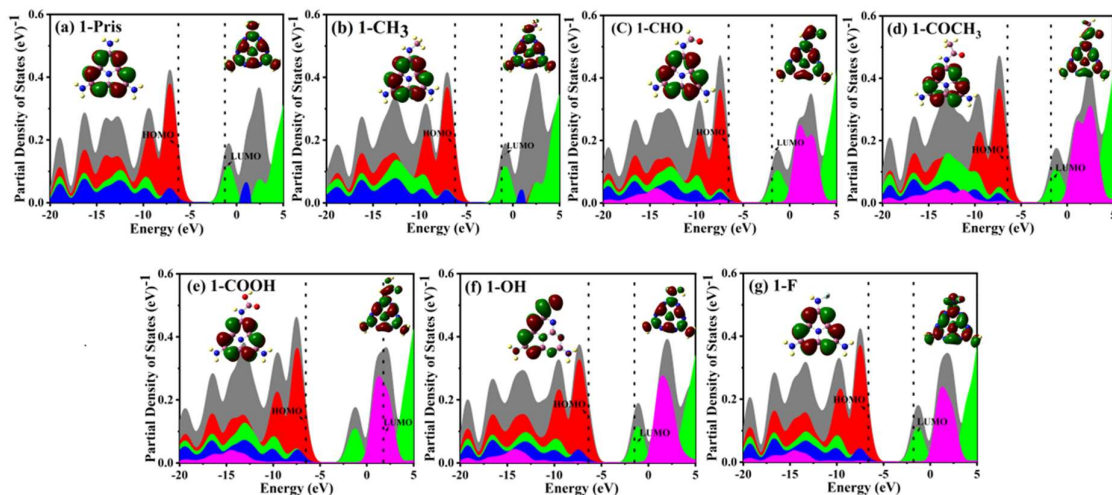

Figure S2: TDOS and PDOS plots of (a) 1-Pris, (b) 1-CH₃, (c) 1-CHO, (d) 1-COCH₃, (e) 1-COOH, (f) 1-OH, and (g) 1-F structures. Grey represents the TDOS. Red, green, blue, and magenta colors represent the contributions of H, N, C, and O or F atoms, respectively. Corresponding HOMO and LUMO are shown in the inset of each plot.
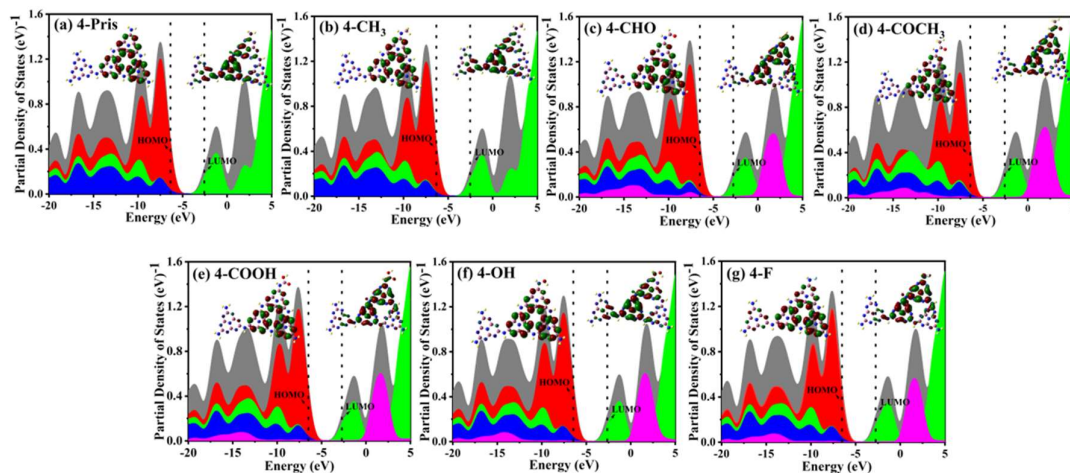

Figure S3: TDOS and PDOS plots of (a) 4-Pris, (b) 4-CH₃, (c) 4-CHO, (d) 4-COCH₃, (e) 4-COOH, (f) 4-OH, and (g) 4-F structures. Grey represents the TDOS. Red, green, blue, and magenta colors represent the contributions of H, N, C, and O or F atoms, respectively. Corresponding HOMO and LUMO are shown in the inset of each plot.

Figure S4: TDOS and PDOS plots of (a) 5-Pris, (b) 5-CH$_3$, (c) 5-CHO, (d) 5-COCH$_3$, (e) 5-COOH, (f) 5-OH, and (g) 5-F structures. Grey represents the TDOS. Red, green, blue, and magenta colors represent the contributions of H, N, C, and O or F atoms, respectively. Corresponding HOMO and LUMO are shown in the inset of each plot.
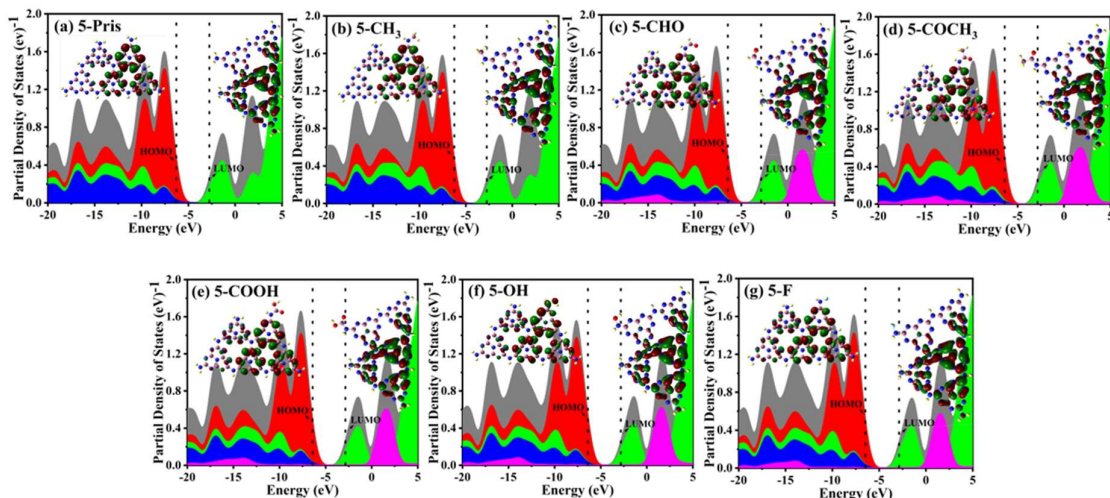

Figure S5: TDOS and PDOS plots of (a) 6-Pris, (b) 6-CH$_3$, (c) 6-CHO, (d) 6-COCH$_3$, (e) 6-COOH, (f) 6-OH, and (g) 6-F structures. Grey represents the TDOS. Red, green, blue, and magenta colors represent the contributions of H, N, C, and O or F atoms, respectively. Corresponding HOMO and LUMO are shown in the inset of each plot.
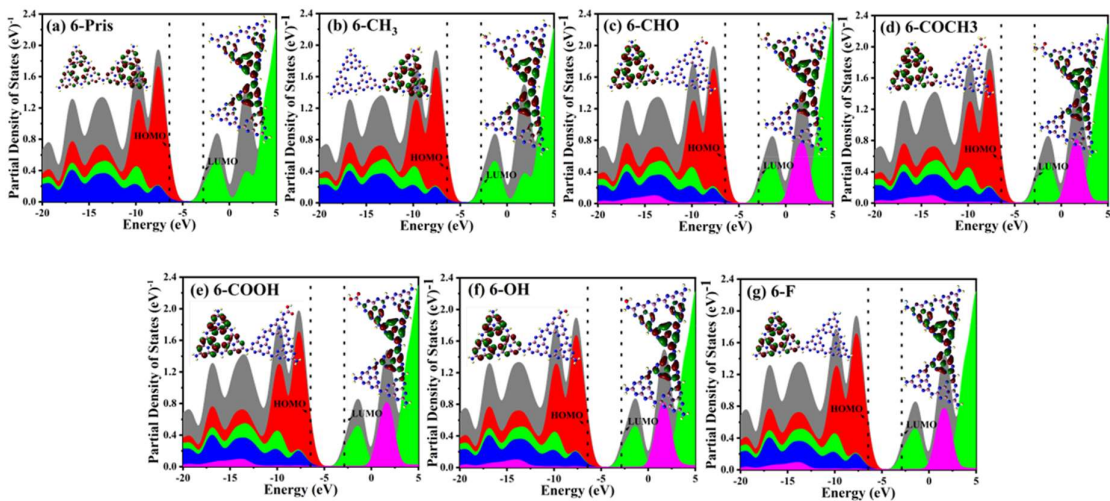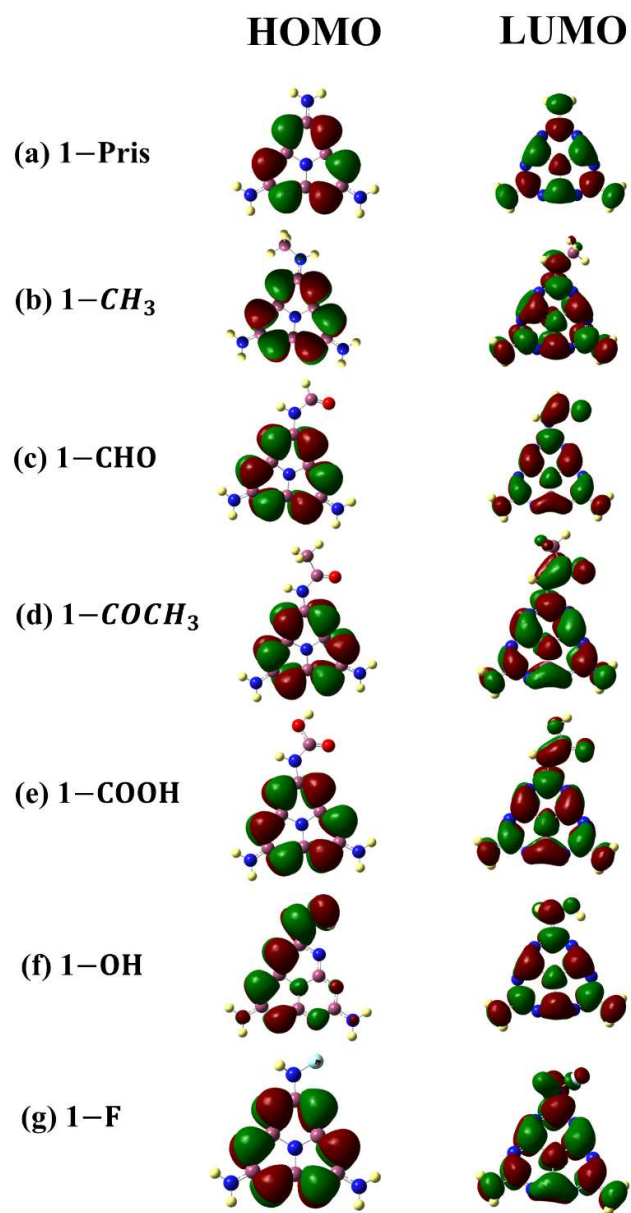
HOMO　　**LUMO**

(a) 1−Pris

(b) 1−CH_3

(c) 1−CHO

(d) 1−$COCH_3$

(e) 1−COOH

(f) 1−OH

(g) 1−F

Figure S6: HOMO and LUMO plots for the 1-X structures obtained using HSE06 functional.

D. UV-vis absorption spectra, TD-DFT wave functions, and spatial distribution of photo-induced electrons and holes
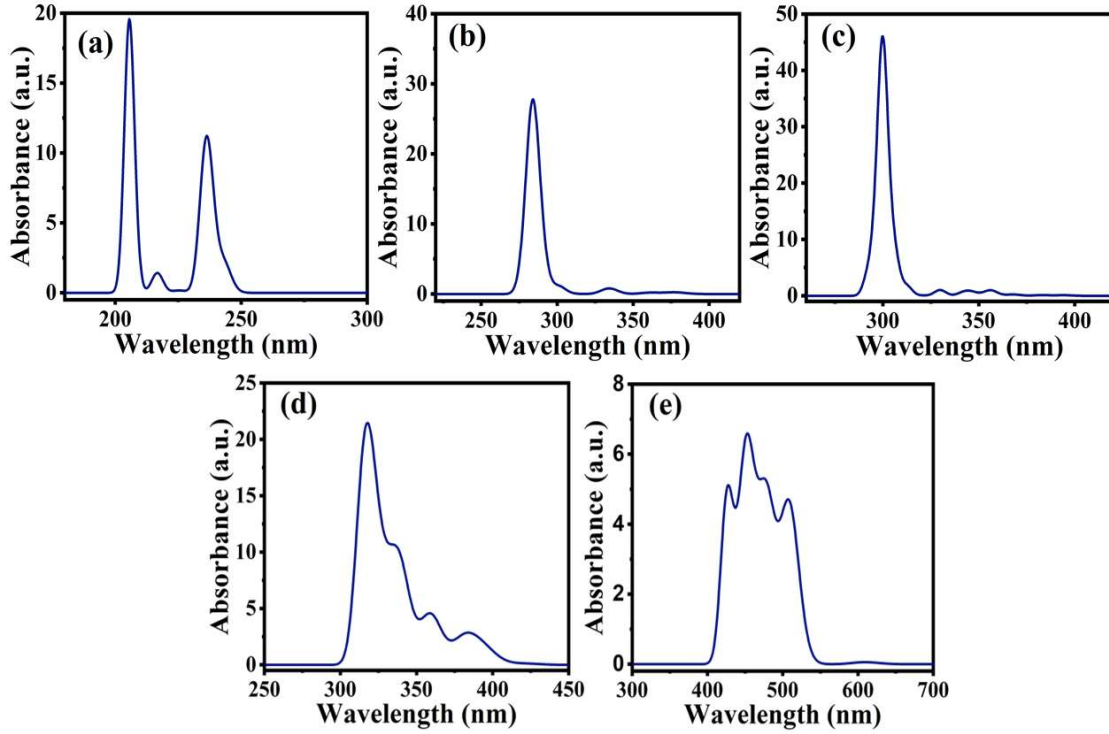

Figure S7: UV-vis absorption spectra of (a) 1-Pris, (b) 3-Pris, (c) 4-Pris, (d) 5-Pris, and (e) 6-Pris structures.

Table S2: TD-DFT wave functions, excitation energies (E_x) and oscillator strengths (f) corresponding to the most intense peaks in the absorption spectra of "1-X" hg-C_3N_4 Qds. Below a configuration H-m $\rightarrow$ L+n implies a single excitation from the HOMO - m orbital to the LUMO + n orbital.

Structure	State	Configuration	Coefficient	E_x(eV)	f
1-Pris	20^1A	$\lvert H-4 \rightarrow L+1\rangle$	0.5092	6.03 (205 nm)	1.02
		$\lvert H-2 \rightarrow L+1\rangle$	-0.2173		
		$\lvert H-1 \rightarrow L+1\rangle$	0.2170		
1-CH$_3$	12^1A	$\lvert H-1 \rightarrow L+1\rangle$	0.3398	5.95 (208 nm)	0.35
		$\lvert H-1 \rightarrow L+2\rangle$	0.4118		
		$\lvert H-4 \rightarrow L\rangle$	0.3195		
1-CHO	20^1A	$\lvert H-3 \rightarrow L+2\rangle$	0.5623	5.93 (209 nm)	0.80
		$\lvert H-1 \rightarrow L+1\rangle$	-0.3170		
		$\lvert H \rightarrow L+1\rangle$	0.1383		
1-COCH$_3$	13^1A	$\lvert H-6 \rightarrow L\rangle$	0.6549	5.41 (229 nm)	0.56
		$\lvert H-3 \rightarrow L+1\rangle$	0.1732		
		$\lvert H-1 \rightarrow L+1\rangle$	0.1095		

Structure	State	Configuration	Coefficient	E_x(eV)	f
1-COOH	14^1A	$\lvert H-6 \to L\rangle$	0.6276	5.56 (223 nm)	0.57
		$\lvert H-2 \to L+1\rangle$	0.2950		
1-OH	10^1A	$\lvert H-1 \to L+1\rangle$	0.3678	5.20 (238 nm)	0.37
		$\lvert H-1 \to L+2\rangle$	-0.3248		
		$\lvert H-2 \to L\rangle$	-0.2989		
1-F	20^1A	$\lvert H-2 \to L+2\rangle$	0.3665	5.96 (208 nm)	1.00
		$\lvert H-4 \to L+2\rangle$	0.3243		
		$\lvert H-5 \to L+2\rangle$	0.3056		

Table S3: The same information as in Table S2 but for the "3-X" hg-C$_3$N$_4$ QDs.

Structure	State	Configuration	Coefficient	E_x(eV)	f
3-Pris	14^1A	$\lvert H-6 \to L\rangle$	0.4449	4.36 (284 nm)	0.97
		$\lvert H-5 \to L+1\rangle$	-0.3542		
		$\lvert H-4 \to L\rangle$	0.2579		
3-CH$_3$	16^1A	$\lvert H-6 \to L\rangle$	0.3937	4.38 (283 nm)	0.50
		$\lvert H-5 \to L\rangle$	0.2959		
		$\lvert H-6 \to L+1\rangle$	-0.2192		
3-CHO	16^1A	$\lvert H-3 \to L+1\rangle$	0.3043	4.31	0.85
		$\lvert H-5 \to L\rangle$	0.2917	(287.7 nm)	
		$\lvert H-6 \to L+1\rangle$	0.2527		
3-COCH$_3$	16^1A	$\lvert H-6 \to L+1\rangle$	0.3656	4.32 (287 nm)	0.90
		$\lvert H-3 \to L+1\rangle$	-0.3040		
		$\lvert H-7 \to L\rangle$	-0.2778		
3-COOH	15^1A	$\lvert H \to L+3\rangle$	0.3280	4.31 (288 nm)	0.40
		$\lvert H-6 \to L\rangle$	0.3004		
		$\lvert H-3 \to L+1\rangle$	-0.2949		
3-OH	17^1A	$\lvert H-5 \to L\rangle$	0.3578	4.36 (284 nm)	0.80
		$\lvert H-6 \to L\rangle$	-0.2961		
		$\lvert H-6 \to L+1\rangle$	-0.2479		
3-F	14^1A	$\lvert H \to L+3\rangle$	0.3101	4.31 (287 nm)	0.50
		$\lvert H-5 \to L+1\rangle$	-0.2843		
		$\lvert H-4 \to L\rangle$	-0.2595		

Table S4: The same information as in Table S2 but for the "4-X" hg-C$_3$N$_4$ QDs.

Structure	State	Configuration	Coefficient	E_x(eV)	f
4-Pris	16^1A	$\lvert H-6 \to L+1\rangle$	0.2821	4.14 (299 nm)	0.70
		$\lvert H-6 \to L\rangle$	0.2185		
		$\lvert H-7 \to L\rangle$	-0.1951		
4-CH$_3$	18^1A	$\lvert H-7 \to L\rangle$	0.4045	4.16 (298 nm)	1.3
		$\lvert H-8 \to L\rangle$	0.3146		
		$\lvert H-5 \to L\rangle$	-0.2475		
4-CHO	17^1A	$\lvert H-4 \to L\rangle$	0.3253	4.12 (301 nm)	0.80
		$\lvert H-6 \to L+1\rangle$	0.2513		
		$\lvert H \to L+3\rangle$	0.2075		
4-COCH$_3$	17^1A	$\lvert H-4 \to L\rangle$	0.2551	4.12 (301 nm)	1.00
		$\lvert H-7 \to L+1\rangle$	0.2178		
		$\lvert H-6 \to L+1\rangle$	-0.2066		

Structure	State	Configuration	Coefficient	E_x(eV)	f
4-COOH	16^1A	$\|H-6 \rightarrow L+1\rangle$	0.3328	4.11 (301 nm)	1.30
		$\|H-6 \rightarrow L\rangle$	0.2526		
		$\|H-4 \rightarrow L\rangle$	-0.2338		
4-OH	18^1A	$\|H-7 \rightarrow L\rangle$	0.3569	4.15 (298 nm)	1.26
		$\|H-6 \rightarrow L\rangle$	-0.2712		
		$\|H-9 \rightarrow L\rangle$	0.2109		
4-F	16^1A	$\|H-6 \rightarrow L+1\rangle$	0.3139	4.11 (301 nm)	1.20
		$\|H-4 \rightarrow L\rangle$	-0.2616		
		$\|H-6 \rightarrow L\rangle$	0.2527		

Table S5: The same information as in Table S2 but for the "5-X" hg-C_3N_4 QDs.

Structure	State	Configuration	Coefficient	E_x(eV)	f
5-Pris	15^1A	$\|H-5 \rightarrow L+1\rangle$	0.3091	3.90 (318 nm)	0.02
		$\|H-6 \rightarrow L+1\rangle$	-0.2092		
		$\|H-5 \rightarrow L\rangle$	-0.1928		
5-CH_3	14^1A	$\|H-6 \rightarrow L\rangle$	0.3071	3.90 (318 nm)	0.03
		$\|H-6 \rightarrow L+1\rangle$	-0.2400		
		$\|H-5 \rightarrow L+1\rangle$	-0.1996		
5-CHO	17^1A	$\|H-1 \rightarrow L+3\rangle$	0.3216	3.92 (316 nm)	0.02
		$\|H \rightarrow L+3\rangle$	0.2912		
		$\|H-5 \rightarrow L\rangle$	0.2832		
5-$COCH_3$	16^1A	$\|H-10 \rightarrow L\rangle$	-0.2801	3.92 (316 nm)	0.03
		$\|H-3 \rightarrow L+2\rangle$	-0.2305		
		$\|H-5 \rightarrow L+1\rangle$	-0.2196		
5-COOH	18^1A	$\|H-10 \rightarrow L\rangle \rightarrow$	0.3228	3.93 (315 nm)	0.04
		$\|H \rightarrow L+3\rangle$	0.2362		
		$\|H-6 \rightarrow L\rangle$	0.2345		
5-OH	13^1A	$\|H \rightarrow L+2\rangle$	0.4466	3.88 (319 nm)	0.04
		$\|H-2 \rightarrow L+1\rangle$	-0.2895		
		$\|H-3 \rightarrow L+1\rangle$	-0.2504		
5-F	18^1A	$\|H-10 \rightarrow L\rangle$	0.3333	3.93 (315 nm)	0.05
		$\|H-6 \rightarrow L\rangle$	0.2387		
		$\|H \rightarrow L+3\rangle$	0.2174		

Table S6: The same information as in Table S2 but for the "6-X" hg-C_3N_4 QDs.

Structure	State	Configuration	Coefficient	E_x(eV)	f
6-Pris	7^1A	$\|H-1 \rightarrow L\rangle$	0.3960	2.72 (455 nm)	0.02
		$\|H-3 \rightarrow L\rangle$	-0.3583		
		$\|H-2 \rightarrow L\rangle$	-0.3026		
6-CH_3	13^1A	$\|H-5 \rightarrow L+2\rangle$	0.3067	3.82 (324 nm)	0.08
		$\|H-4 \rightarrow L+1\rangle$	-0.2741		
		$\|H-5 \rightarrow L\rangle$	-0.2423		
6-CHO	12^1A	$\|H-5 \rightarrow L+1\rangle$	0.4625	3.76 (330 nm)	0.05
		$\|H-1 \rightarrow L+1\rangle$	0.2697		
		$\|H-3 \rightarrow L+1\rangle$	-0.2448		

6-COCH$_3$	12^{1}A	$\lvert H-5 \rightarrow L+1 \rangle$	0.3116	3.74 (331 nm)	0.06
		$\lvert H-1 \rightarrow L+1 \rangle$	0.4405		
		$\lvert H-8 \rightarrow L+1 \rangle$	0.1629		
6-COOH	12^{1}A	$\lvert H-5 \rightarrow L+1 \rangle$	0.4481	3.70 (335 nm)	0.06
		$\lvert H-1 \rightarrow L+1 \rangle$	0.3037		
		$\lvert H-3 \rightarrow L+1 \rangle$	-0.2227		
6-OH	13^{1}A	$\lvert H-1 \rightarrow L+1 \rangle$	0.3756	3.74 (332 nm)	0.14
		$\lvert H-1 \rightarrow L+3 \rangle$	-0.2859		
		$\lvert H-2 \rightarrow L+2 \rangle$	-0.2452		
6-F	12^{1}A	$\lvert H-5 \rightarrow L+1 \rangle$	0.4108	3.72 (333 nm)	0.06
		$\lvert H-1 \rightarrow L+1 \rangle$	0.2965		
		$\lvert H-3 \rightarrow L+1 \rangle$	-0.2395		

Table S7: The oscillator strengths (f) and excitation energies (E_x) corresponding to the first excited state (1^{1}A) with the TD-DFT wave function dominated by the HOMO (H) → LUMO (L) excitation.

Structure	E_x (eV)	f
1-Pris	4.06	0.0000
1-CH$_3$	4.09	0.0003
1-CHO	3.79	0.0097
1-COCH$_3$	3.83	0.0079
1-COOH	3.85	0.0066
1-OH	4.07	0.0055
1-F	4.07	0.0045
3-Pris	3.26	0.0005
3-CH$_3$	3.24	0.0004
3-CHO	3.16	0.0011
3-COCH$_3$	3.18	0.0013
3-COOH	3.18	0.0015
3-OH	3.23	0.0007
3-F	3.20	0.0014
4-Pris	3.14	0.0032
4-CH$_3$	3.15	0.0031
4-CHO	3.10	0.0000
4-COCH$_3$	3.11	0.0002
4-COOH	3.11	0.0003
4-OH	3.15	0.0020
4-F	3.12	0.0003
5-Pris	2.95	0.0007
5-CH$_3$	2.94	0.0006
5-CHO	2.95	0.0009
5-COCH$_3$	2.95	0.0008
5-COOH	2.95	0.0009

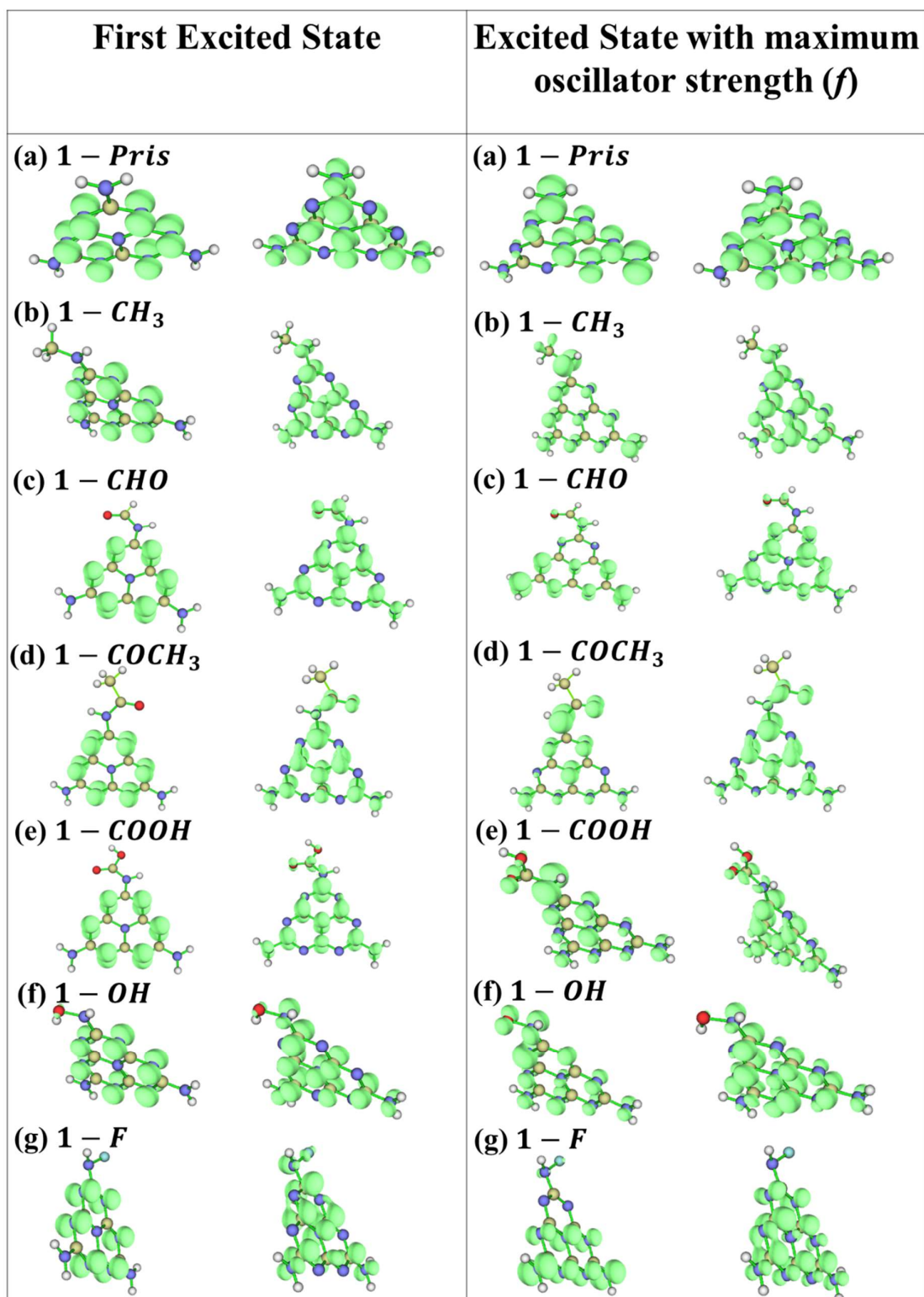|		
5-OH	2.95	0.0007
5-F	2.95	0.0010
6-Pris	2.03	0.0003
6-CH$_3$	3.07	0.0037
6-CHO	3.06	0.0022
6-COCH$_3$	3.06	0.0026
6-COOH	3.06	0.0025
6-OH	3.07	0.0034
6-F	3.06	0.0025

Figure S8: Spatial distribution (shown in green) of the photo-induced electrons (right) and holes (left) at the first excited state and the excited state with maximum oscillator strength for the 1-X structures. Here yellow, blue, grey, red, and cyan spheres represent the carbon, nitrogen, hydrogen, oxygen, and fluorine atoms, respectively.
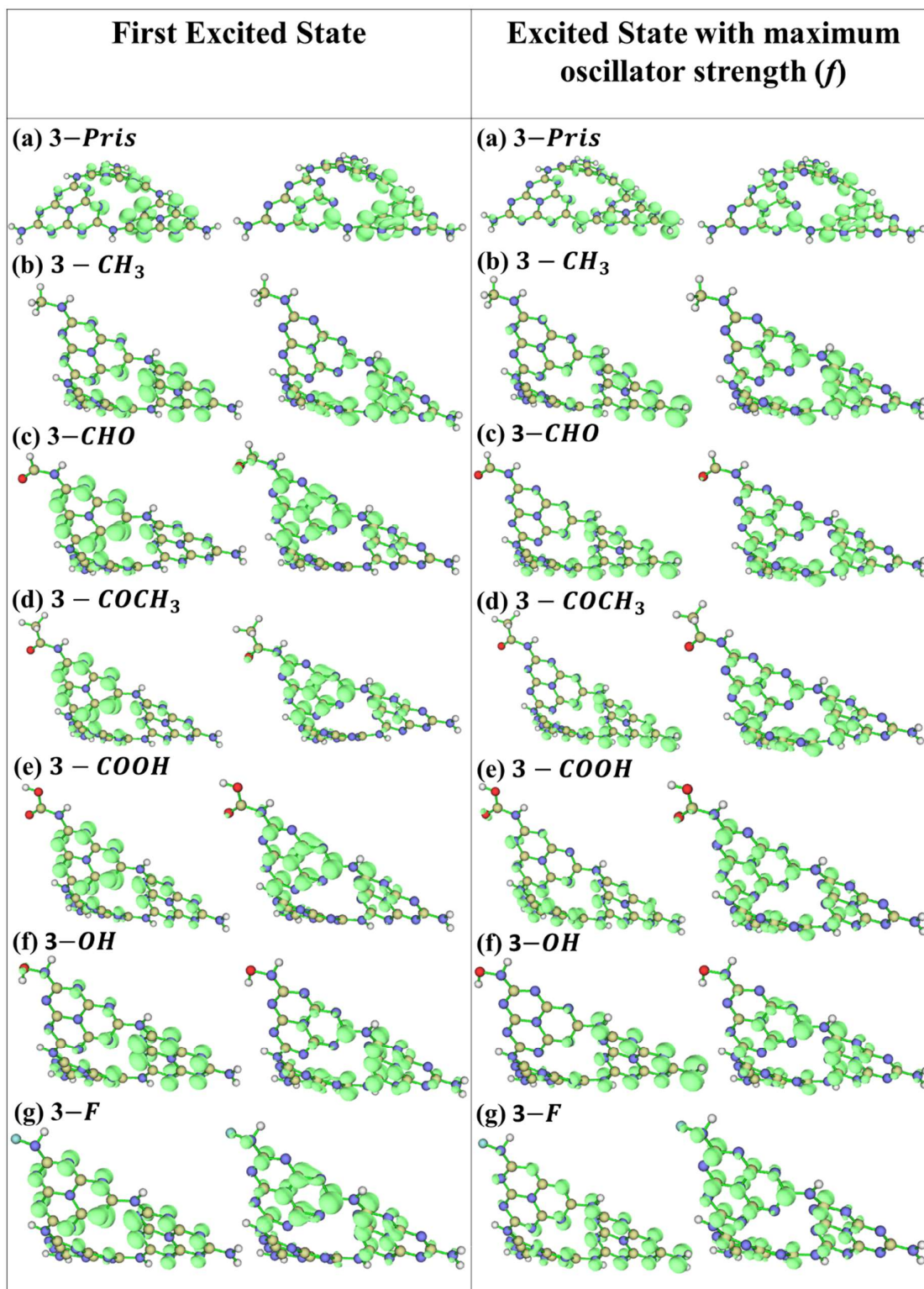
First Excited State	Excited State with maximum oscillator strength (*f*)

Figure S9: Spatial distribution (shown in green) of the photo-induced electrons (right) and holes (left) at the first excited state and the excited state with maximum oscillator strength for the 3-X structures. Here yellow, blue, grey, red, and cyan spheres represent the carbon, nitrogen, hydrogen, oxygen, and fluorine atoms, respectively.
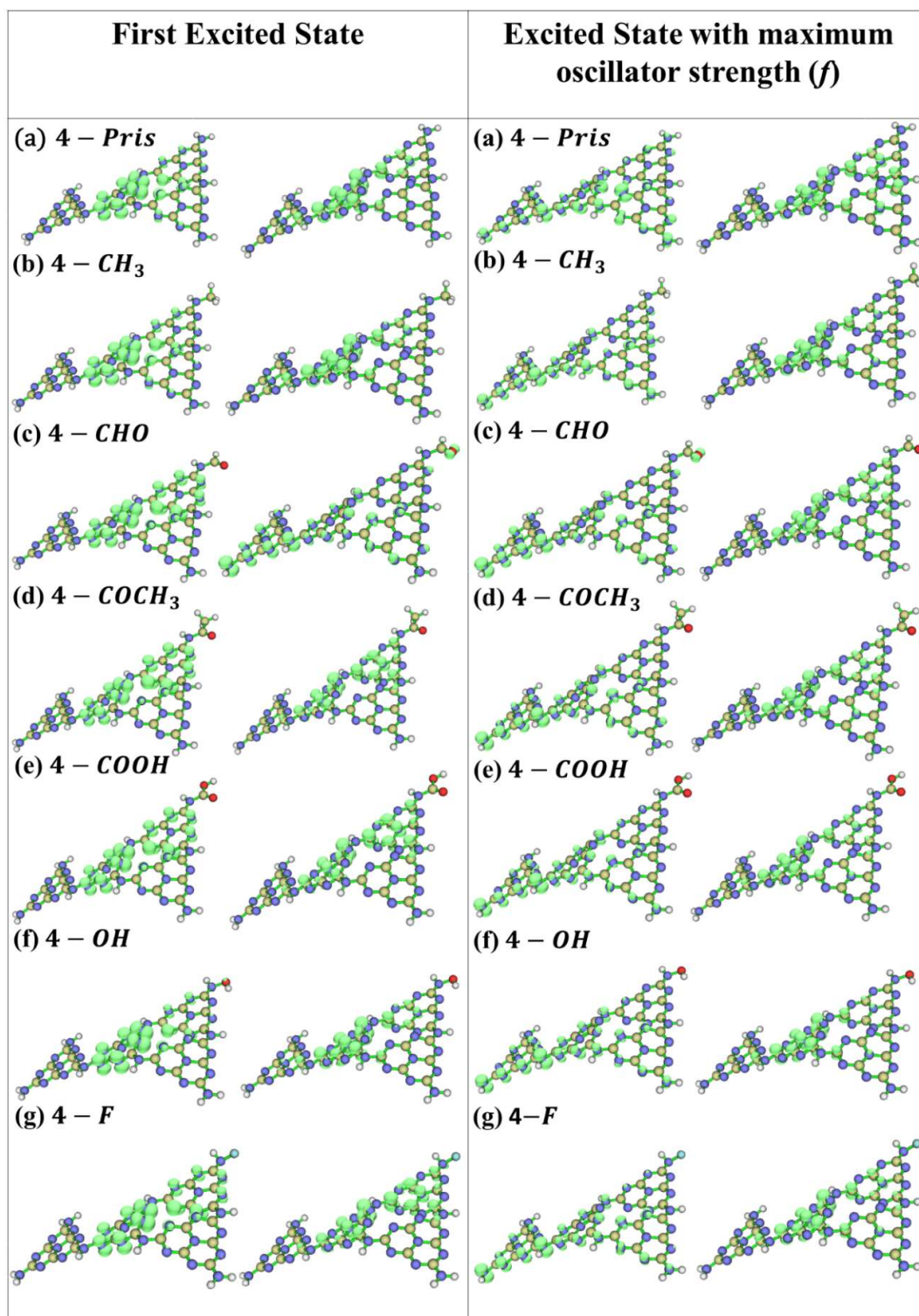
First Excited State	Excited State with maximum oscillator strength (*f*)

(a) 4 − Pris

(b) 4 − CH_3

(c) 4 − CHO

(d) 4 − $COCH_3$

(e) 4 − COOH

(f) 4 − OH

(g) 4 − F

Figure S10: Spatial distribution (shown in green) of the photo-induced electrons (right) and holes (left) at the first excited state and the excited state with maximum oscillator strength for the 4-X structures. Here yellow, blue, grey, red, and cyan spheres represent the carbon, nitrogen, hydrogen, oxygen, and fluorine atoms, respectively.
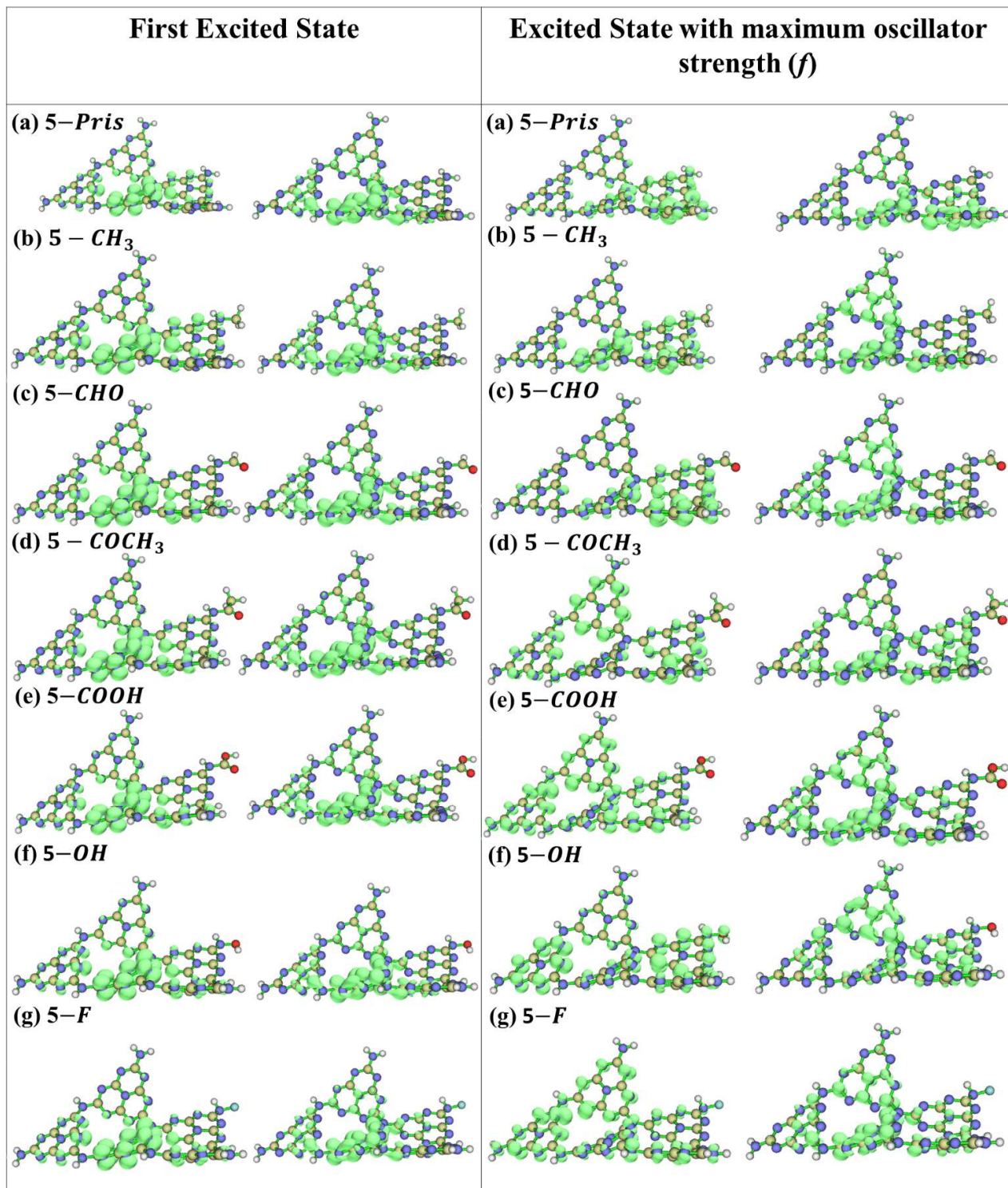
First Excited State	Excited State with maximum oscillator strength (f)
(a) 5−Pris	**(a) 5−Pris**
(b) 5 − CH₃	**(b) 5 − CH₃**
(c) 5−CHO	**(c) 5−CHO**
(d) 5 − COCH₃	**(d) 5 − COCH₃**
(e) 5−COOH	**(e) 5−COOH**
(f) 5−OH	**(f) 5−OH**
(g) 5−F	**(g) 5−F**

Figure S11: Spatial distribution (shown in green) of the photo-induced electrons (right) and holes (left) at the first excited state and the excited state with maximum oscillator strength for the 5-X structures. Here yellow, blue, grey, red, and cyan spheres represent the carbon, nitrogen, hydrogen, oxygen, and fluorine atoms, respectively.
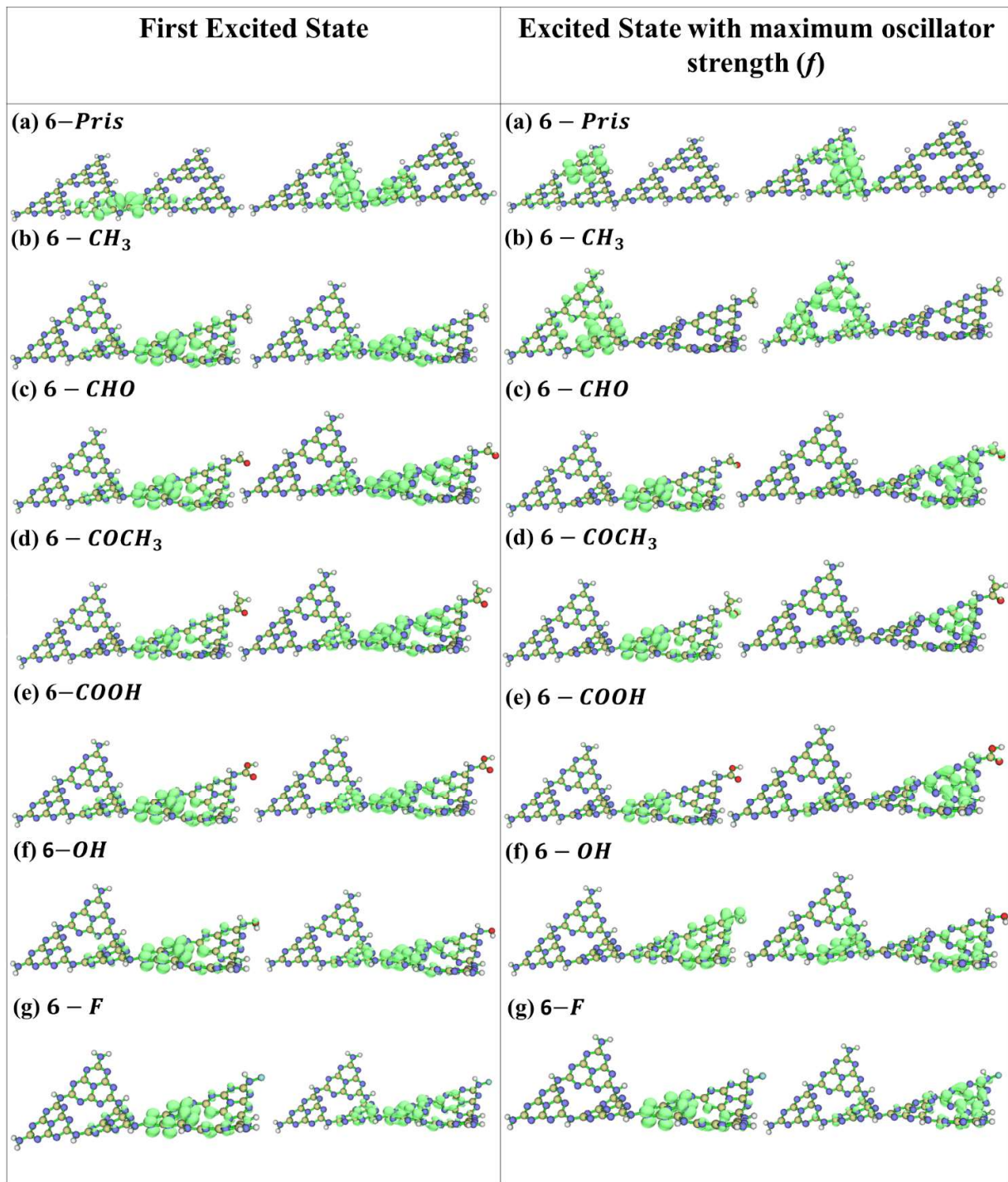
Figure S12: Spatial distribution (shown in green) of the photo-induced electrons (right) and holes (left) at the first excited state and the excited state with maximum oscillator strength for the 6-X structures. Here golden, blue, grey, red, and cyan spheres represent the carbon, nitrogen, hydrogen, oxygen, and fluorine atoms, respectively.